Spin-wave anomalies in reentrant spin glasses of $Au_{1-x}Fe_x$ alloys

B. Hennion, M. Hennion, and I. Mirebeau
Laboratoire Léon Brillouin (CEA-CNRS), CEN-Saclay, 91191 Gif-sur-Yvette Cedex, France

M. Alba
Institut Laue Langevin, 38 042 Grenoble Cedex, France
(Received 29 November 1994)

Inelastic-neutron-scattering measurements have been performed on two reentrant spin glasses (RSG's) of $Au_{1-x}Fe_x$ ($x=0.19,0.21$). For decreasing temperature, the spin-wave stiffness constant D shows a maximum then decreases. Concomitantly, the damping Γ increases, as has previously been observed in many RSG's. At still lower temperatures, these variations of D and Γ are reversed. The characteristic temperature where this new regime occurs increases with increasing x, thereby showing its direct relation with the frustration of the system. We discuss the observed behavior by considering a model of scattering of spin waves by weak antiferromagnetic bonds.

INTRODUCTION

Reentrant spin glasses (RSG's) are disordered magnetic systems where the strong increase of the low-field magnetization and its subsequent decrease at low temperature suggest the following sequence of transitions: paramagnetic→ferromagnetic→spin glass. Such behavior is caused by the frustration corresponding to the competition between ferromagnetic (F) and antiferromagnetic (AF) coupling, with a dominant ferromagnetic coupling. It depends on the concentration (x) and eventually on the thermal heat treatment of the alloys. Examples are found both in insulating compounds with short-range interactions (EuSrS,[1] Fe spinels[2]) and in metallic ones ($Au_{1-x}Fe_x$,[3] $Ni_{1-x}Mn_x$,[4] $Fe_{1-x}Cr_x$,[5] amorphous Fe and Ni compounds[6–8]).

Three typical neutron experiments have usually been performed: small-angle neutron scattering (SANS), which probes inhomogeneities on a 10–500 Å scale, neutron depolarization experiments, which probe static inhomogeneities on the μm scale, and inelastic neutron scattering, which provides the characteristic excitations of these systems. The first two experiments have shown the existence of two characteristic length scales. On one hand, small-angle neutron scattering reveals the onset of inhomogeneities on a 10–50 Å scale at a characteristic temperature between T_c and T_f. On applying a magnetic field, they can be characterized as transverse spin correlations.[9] On the other hand, in most cases, the study of depolarization of the transmitted neutron beam at T_c, indicates the persistence of the size of domains down to the lowest temperatures.[10] It was therefore concluded that, at low temperature, the ferromagnetic long-range order coexists with frozen transverse spin components. Consequently, the decrease of the low-field magnetization is attributed to a pinning of the domain walls.

In contradiction with this picture, most studies of spin waves have supported the picture of a disappearance of the magnetization on a more microscopic scale. The spin-wave stiffness constant starts to increase when T decreases below T_c, shows a maximum (between T_c and T_f), and then decreases, following roughly the decrease of the magnetization.[11–14] This behavior also agrees with a study of a $Au_{0.81}Fe_{0.19}$ alloy performed in a limited temperature range by Murani.[15] Very surprisingly, in NiMn (Ref. 16) and FeMn (Refs. 17,18) these two regimes are followed at still lower temperature by a third one, where $D(T)$ increases again, showing a minimum. Hence, at least for these two alloys, there is no relationship between $D(T)$ and $M(T)$. In this context a study of $Au_{1-x}Fe_x$ in the low-temperature spin-glass state was especially interesting. Several questions are raised. Does the different behavior of spin waves in RSG's arise from the chemical nature of the system (Mn could play a special role), from the use of two distinct models to analyze the spin waves (as Murani[15] suggested), or from experimental difficulties? Indeed, at low temperature where they become less populated, spin waves coexist with a huge elastic intensity (the SANS intensity mentioned above) so that very long counting rates and an excellent energy resolution are required.

$Au_{1-x}Fe_x$ is one of the most studied RSG's. Its phase diagram was established by Sarkissian.[3] SANS measurements were performed by Murani *et al.*[19] Peculiar anomalies of the magnetic Bragg peak intensity were observed by Murani.[20] Neutron depolarization measurements at $x=0.19$ show[21] a very slight decrease of the domain magnetization at low temperature. More recently, the critical region ($T \simeq T_c$) has also been investigated by Mössbauer spectroscopy[22] and neutron inelastic studies.[23] The inelastic study of Murani,[15] in $Au_{1-x}Fe_x$ ($x=0.19$) down to 35 K, shows the two regimes previously described. We present here a complete study of the $x=0.19$ alloy (140 K $< T <$ 10 K) together with a study of the $x=0.21$ alloy. Indeed, in the lowest temperature range ($T<30$ K), we observe an increase of $D(T)$, whatever the model used for the analysis. By varying the Fe concentration, we change the value of the mean fer-

romagnetic interaction, thereby showing that the observed anomalies are closely related to the magnetic frustration. After describing the experimental results, we discuss the observed behavior by considering a model of scattering of spin waves by weak antiferromagnetic bonds.

EXPERIMENTAL RESULTS

Two slices of dimension $0.8\times1\times3$ cm^3 were cut from single crystals of $Au_{1-x}Fe_x$ with $x=0.19$ and 0.21. They were annealed at 600 °C for 5 h and quenched into water. From the temperature dependence of the dc susceptibility we determined the characteristic temperatures $T_c=168$ K and $T_f=36$ K ($x=0.19$) and $T_c=192$ K and $T_f=28$ K ($x=0.21$), in close agreement with the diagram of Sarkissian.[3] The neutron experiments were carried out on the IN14 spectrometer at the Institut Laue Langevin, using the cold neutron source. At each temperature, four scattering vectors q were studied at nominal values of 0.04, 0.05, 0.065, and 0.075 Å^{-1}. For these increasing q values, we used increasing wave vectors k_i of 1.05, 1.12, and 1.25 Å^{-1}. This corresponds to energy-resolution linewidths [full width at half maximum (FWHM)] of 0.0056, 0.0083, and 0.014 THz, respectively. The resolution function was checked by a vanadium spectrum. The raw spectra were corrected for the scattering of the sample holder, taking the sample absorption into account.

Since spin waves have rather low energies, their thermal population factor is approximately kT. In order to keep the same level of accuracy for all temperatures, we started from high temperatures where the spin waves are well defined, and, when lowering T, we increased the counting rate of the monitor M_0. Some energy spectra for $x=0.19$ are reported in Fig. 1. At high temperatures, the spin-wave maxima are easily detected, being far away from the $\omega=0$ central peak (nuclear contribution). With decreasing temperature, the spin-wave energy shows a maximum, then softens and becomes damped, so that the inelastic peaks are barely observable around 40 K. However, in the extended temperature range ($T<35$ K), the spin-wave peaks now move away from the elastic one. This low-temperature behavior is observable even though the central peak considerably increases between 40 and 10 K, thanks to a good energy resolution and a sufficient counting time. Similar results are observed for $x=0.21$ (Fig. 2).

For a conventional ferromagnet, the transverse spin correlation function (spin-wave excitations) can be expressed as

$$S(q,\omega)\propto\omega(n(\omega)+1)\chi_0^t(q)F(q,\omega)\ . \qquad (1)$$

Here ω is algebraic, $\hbar=1$, χ_0^t is the static transverse susceptibility, $n(\omega)$ is the Bose factor, and $F(q,\omega)$ the normalized spectral function. $F(q,\omega)$ contains all the information pertinent to the spin dynamics, namely, the dispersion law $\omega_q=Dq^2$ (or $\omega_q=Dq^2+\Delta$ when introducing a gap) and the damping Γ_q. Since no specific theory exists for such disordered systems, we have used for $F(q,\omega)$ two empirical forms similarly to previous works:[15,18] the double Lorentzian (DL) and the damped harmonic oscillator (DHO) models. Both models have their limitations. As shown by Murani for FeAl,[15] the DL model yields departures from the expected parabolic

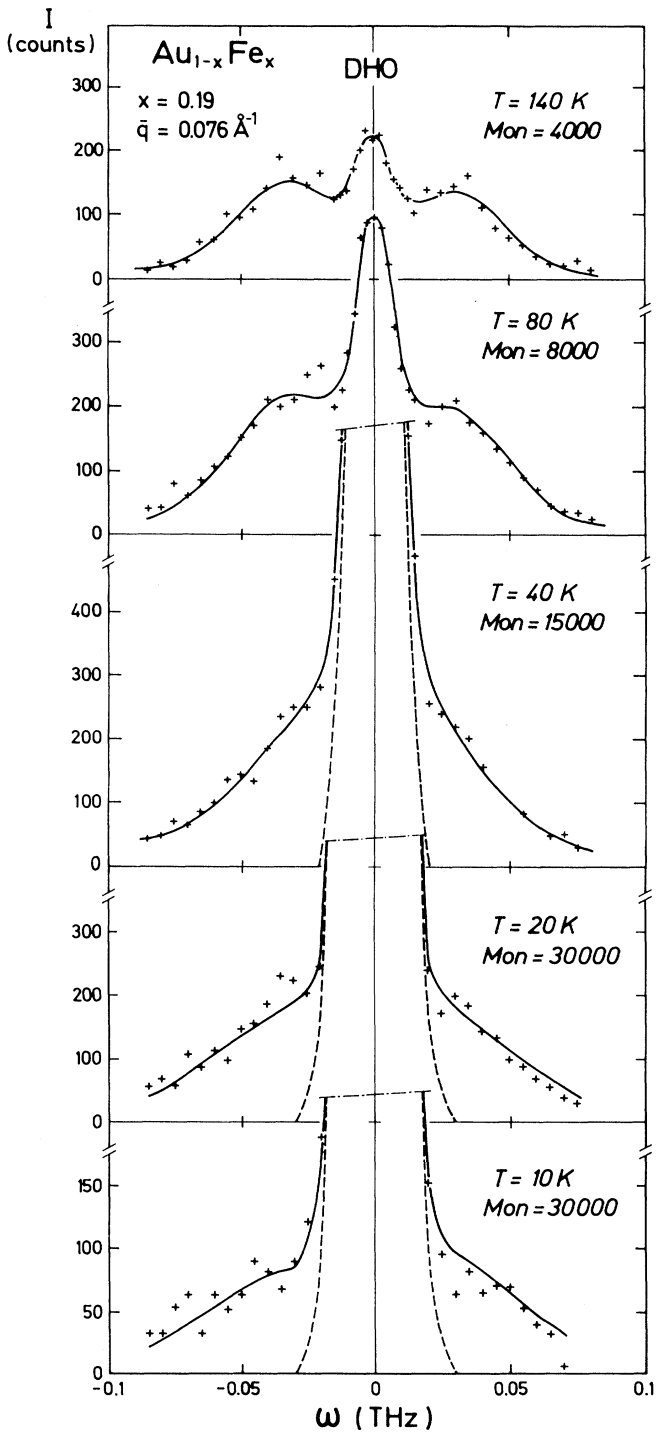

FIG. 1. Examples of fitted corrected data at several temperatures and $q=0.076$ Å^{-1} for the $x=0.19$ sample. Curves are intensities calculated using the damped harmonic oscillator (DHO) model.

dispersion law at large q. On the other hand, the DHO model, derived to describe phonons close to a structural transition, yields an unphysical limit when Γ_q/ω_q goes to infinity. In their analysis of amorphous a $(Fe_{1-x}Ni_x)$, Erwin *et al.*[13] proposed a modified DHO model, with a renormalized energy $\mathcal{E}_q=(\omega_q^2-\Gamma_q^2)^{0.5}$. This procedure provides values of the spin-wave energies intermediate between the DL and the DHO models. Interestingly, such a formulation corresponds to the model of Lindgard[24] for the excitation spectrum of the paramagnetic state close to T_c, within mode-coupling theory. However, since the site disorder cannot be treated as a thermal disorder,[25] the modified DHO model is also empirical in the present case. The DL and DHO models, identical in the limit $\Gamma=0$, yield for the same quality of fit rather different values of the parameters when the damping is large. This prevents the definition of precise "transition" temperatures which could be compared to those of the phase diagram. However, whatever the model chosen, $D(T)$ exhibits the three dynamic regimes noticed from the raw data, with smooth transitions in between. A detailed analysis is given now.

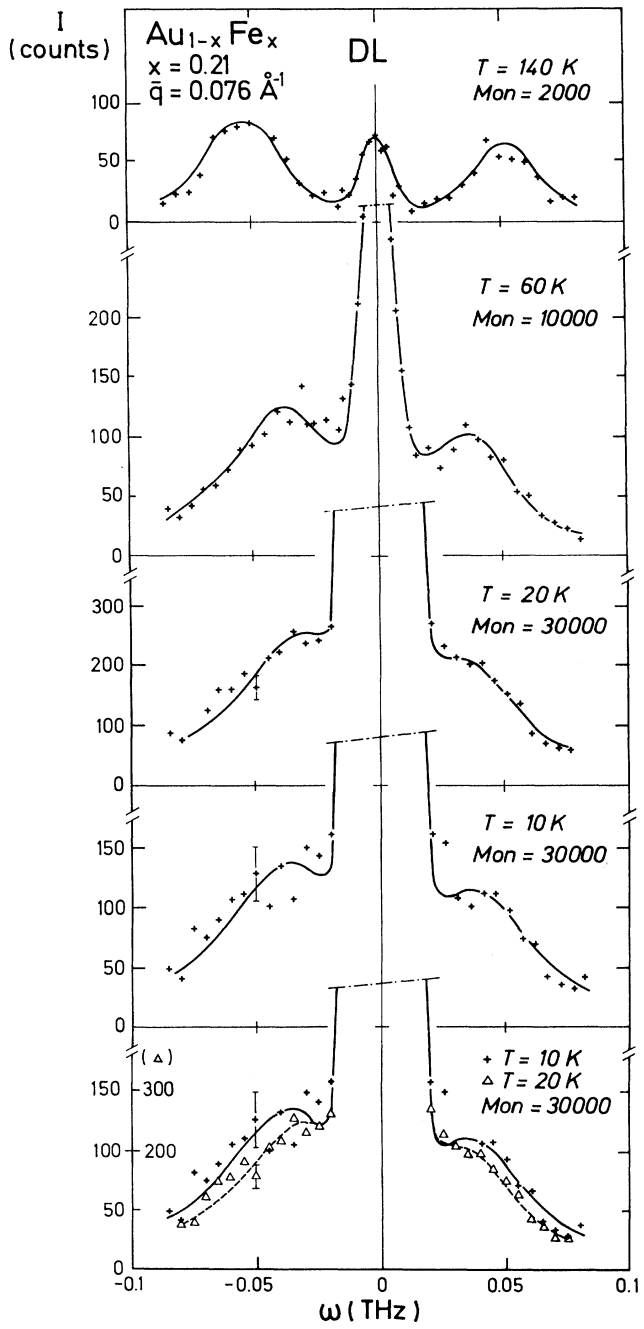

FIG. 2. Examples of fitted corrected data at several temperatures and $q=0.076$ Å^{-1} for the $x=0.21$ sample. Curves are intensities calculated using the double Lorentzian (DL) model.

The total scattered intensity was fitted to the sum of the inelastic component $S(q,\omega)$ defined above and to an elastic component $I_0(q)\delta(\omega)$, convoluted with the resolution function. In a first step, we checked that the overall data were consistent with the usual ferromagnetic description laws, $\omega_q=D^{\text{eff}}q^2$ and $\chi_0^t(q)\propto 1/q^2$. In a second step, we introduced these laws in the fitting procedure to get the best fit for the whole set of q values, thus determining D^{eff}, Γ_q, and $\chi^t(T)=q^2\chi_0^t(q)$. The solid lines through the data of Figs. 1 and 2 correspond to the best fits with the DL model. The parameters derived from this analysis for the two concentrations are reported in Figs. 3 and 4 for the DL model and Figs. 5 and 6 for the DHO one.

The fits were improved by adding an intrinsic gap, $\omega_q=Dq^2+\Delta$. This did not change the overall temperature variations of the parameters, but yielded a D value smaller than D^{eff} especially at low temperature. Concomitantly, the gap Δ was found to increase at low temperatures. The parameters derived from this analysis for the two concentrations are reported in Figs. 3 and 4 for the DL model and Figs. 5 and 6 for the DHO one. The analysis including a gap is shown for the DL model in Fig. 3.

The three regimes are indicated by vertical dashed lines in the $D^{\text{eff}}(T)$ variations. When the temperature decreases below T_c, $D^{\text{eff}}(T)$ first increases, shows a maximum, and then decreases in the lowest temperature range. The $\Gamma_q(T)$ exhibits opposite variations. As previously noticed, the variations of D^{eff} versus T are much more amplified in the DL model than in the DHO one. By contrast, the $\Gamma_q(T)$ variation is much stronger within the DHO model. The modified DHO model, which combines the ω_q and Γ_q variations of the DHO, yields $D^{\text{eff}}(T)$ intermediate between the DL and DHO models (not reported in the figures for simplification).

The q dependence of Γ_q is the same for both models. It can be described by a $\Gamma_q=A(T)q^2$ law. In order to fit Γ_q with a q^4 law, one has to add a q-independent $\Gamma(T,0)$ term which is strongly temperature dependent, resulting in $\Gamma(T,q)=\Gamma(T,0)+B(T)q^4$. Depending on the analysis, $\Gamma(T,0)$ exhibits either a maximum (DHO) or a saturation (DL) at the temperature ($T_{\min}$) where D^{eff} is minimal. Such fits are shown in Fig. 4 for the two concentrations within the DL model.

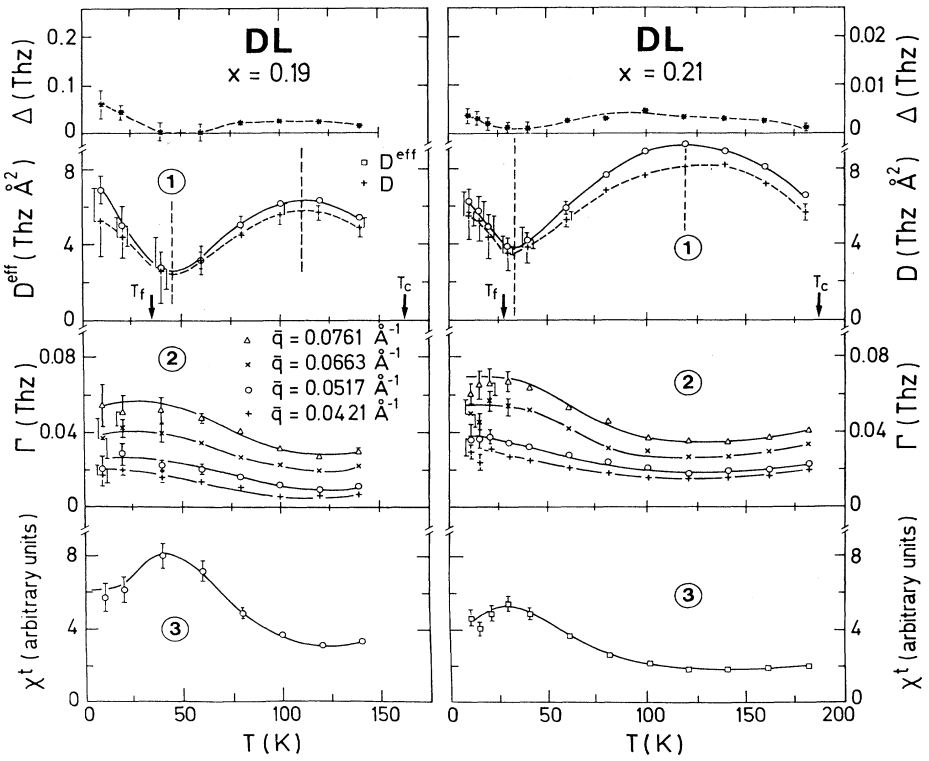

FIG. 3. Comparison between the parameters obtained using the DL model for the $x=0.19$ and $x=0.21$ samples. (1) Temperature dependences of the gap Δ, of the spin-wave stiffness constant D, and the effective stiffness constant D^{eff}. The dashed lines define the three dynamical regimes. The arrows define the characteristic temperatures T_c and T_f. The lines are guides for the eyes. (2) Temperature dependences of the linewidth Γ at several q values. (3) Temperature dependence of the transverse susceptibility $\chi^t(T)$ [$\chi^t(T)=q^2\chi_0^t(T)$].

Assuming a q^2 dependence, the static susceptibility $\chi^t(T)$ behaves in the same way for the two models, clearly showing a maximum at T_{min} for the more frustrated sample ($x=0.19$) [Figs. 3(3) and 5(3)].

The central peak I_0 has the same temperature dependence in both models. The high-temperature value has a nuclear origin. In both samples, I_0 strongly increases below about 80 K, due to an additional magnetic contribution (Fig. 6).

DISCUSSION

In their common temperature range, the results obtained for the $x=0.19$ sample are in excellent agreement with those reported by Murani[15] for the same concentration. Comparing our observations, including the "spin-glass phase" in the two Au-Fe samples, with the previous ones in $Ni_{1-x}Mn_x$ (Ref. 16) and a-$Fe_{1-x}Mn_x$,[17,18] we conclude that these dynamic anomalies are not specific to Mn, but rather reflect a more general effect. Interestingly, in the high-T regime, the maximum value reached by D^{eff} [$\simeq 6$ and 8 THz Å^2 (DL) or $\simeq 8$ and 10 THz Å^2 (DHO) for $x_{\text{Fe}}=0.19$ and 0.21, respectively] scales approximately with T_c. This means that the evolution of D^{eff} with concentration just below T_c must be related to the mean exchange interaction in the alloy. The temperature T_{min} where we observed the minimum of the spin-wave stiffness constant, may also be related to the frustra-

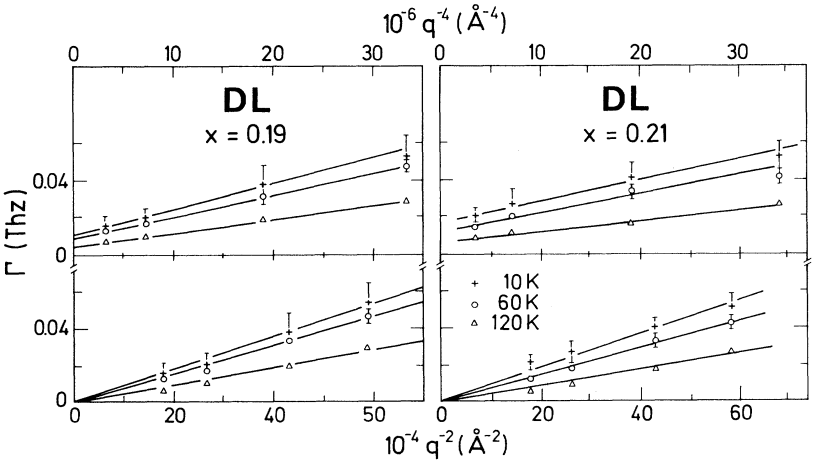

FIG. 4. q dependences of the spin-wave linewidth Γ at several temperatures, using a q^4 scale (upper part) and a q^2 scale (lower part). The solid lines are guides for the eyes.

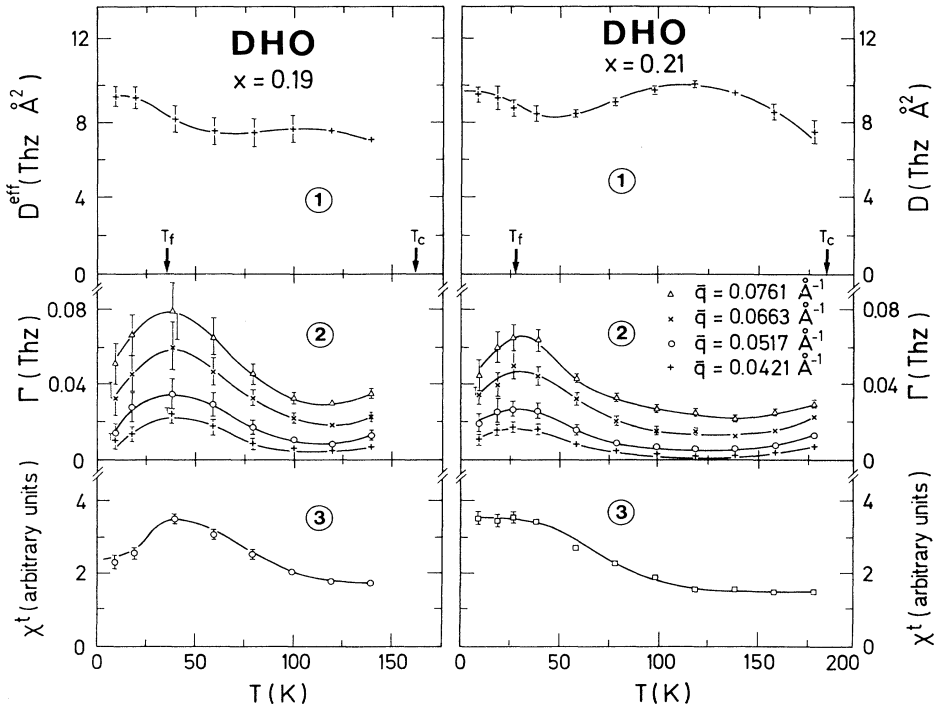

FIG. 5. Comparison between the parameters obtained using the DHO model for the $x=0.19$ and $x=0.21$ samples. (1), (2), and (3) correspond, respectively, to the effective stiffness constant, the linewidth Γ, and the transverse susceptibility $\chi^t(T)$ $[\chi^t(T)=q^2\chi_0^t(T)]$.

tion induced by the competing exchange forces. In Figs. 5 (DL model) and 6 (DHO model), the $D^{\text{eff}}(T)$ curves have been compared on the same figure for $x=0.19$ and 0.21. This clearly shows the shift in temperature of the "third" regime with x. Indeed, the anomalous stiffening observed in both alloys occurs below a temperature $T_{\min}$ which is higher for lower x, corresponding therefore to stronger frustration effects. A similar tendency is found when comparing the evolution of $\Gamma_q(T)$ or $\chi^t(T)$ at the two concentrations (see Figs. 3 and Fig. 5). This $T_{\min}$ value, although ill defined, is slightly higher than T_f (see the arrows of the figures).

Mean-field theory,[25,26] which has been widely invoked to understand the main features of the phase diagram, cannot predict the spatial and time dependences of spin correlations. Therefore we use a completely different approach, namely, the effect of antiferromagnetic bonds dispersed within a ferromagnetic medium. This second model has the advantage of being exactly solvable by quantum mechanics and may be expected to be representative of weakly frustrated systems. Let us summarize it briefly.

In disordered alloys, when an AF interaction is strong enough, it creates a bound or localized state, yielding a decrease of the total spin value, even at zero temperature.[27] In the case of a weak interaction, only a quasilocalized state is created, with no reduction of the spin value.[28] Such states are expected to have a spatial exten-

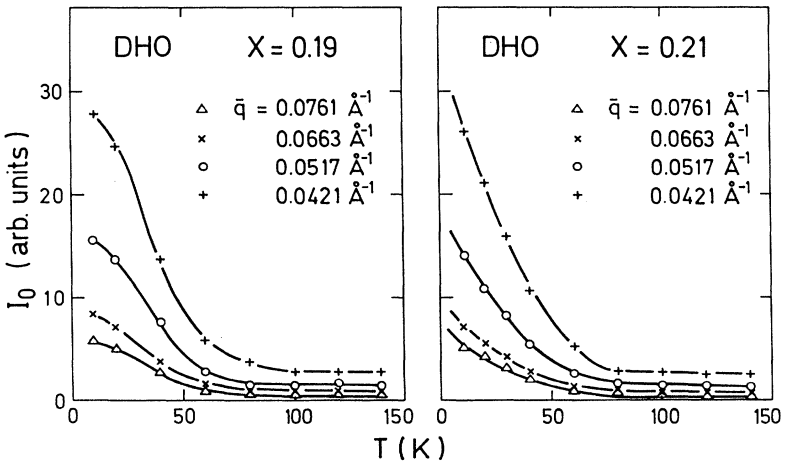

FIG. 6. Temperature dependence of the central peak at several q values and for the two concentrations. The solid line is a guide for the eyes.

sion around the frustrated bond and to be localized at the frustrated bond only for infinitely large antiferromagnetic coupling. Within such a model, it can be shown that the spin waves strongly "repel" each other in the frustrated regions so that multiple occupancy (boson statistics) is forbidden.[28] Therefore the overall spectrum of excitations consists of both propagative spin waves with boson statistics and localized or quasilocalized states with the statistics of two-level systems (TLS's). Within this model, the TLS's have a theoretical basis, whereas in previous ones[29] they were introduced phenomenologically. By averaging the scattering effects of the spin waves over the various frustrated bonds within a perturbative treatment, Korenblit, Maleev, and Shender[30] obtain a complex expression of the spin-wave energy $\omega(q)$, leading to a damping Γ as the imaginary part and to a renormalized stiffness constant D as the real part:

$$\Gamma \propto \frac{Dq^4}{T} \quad \text{and} \quad D - D_0 \propto D_0 \ln\left[\frac{E_m}{2T}\right] . \tag{2}$$

These expressions are valid for a mean energy value E_m of the TLS higher than kT and for $\omega(q) \ll kT$. They lead to a decrease of the stiffness constant D and an increase of the linewidth on decreasing temperature, which could therefore correspond to the second experimentally observed regime. We note, however, that in the above equations D_0 refers to the pure ferromagnetic state and not to the "mean" ferromagnetic state, which occurs below T_c. In addition, the q^4 dependence of Γ_q cannot be ascertained experimentally. If, however, this model holds, it cannot explain the change of behavior of D and Γ in the lowest temperature range. Therefore, this could correspond to a crossover from weak to strong interactions between TLS's. the direct consequence would be the freezing of the spin regions corresponding to a TLS. The dynamical anomalies would be progressively suppressed at low temperature and the spin wave would recover the characteristics of the mean ferromagnetic state as in the high-temperature state.

In this model for weakly frustrated systems, the TLS's have the meaning of "longitudinal" fluctuations and no transverse spin freezing is expected. It provides only a partial description, useful for the spin dynamics. Thanks to our previous SANS observation in an applied field,[9] we can show that the anomalous increase of the central peak intensity I_0 below about 80–90 K in both alloys corresponds to the freezing of the transverse spin component. We recall that spin waves become anomalous below 130 K without any effect at 80 K. In the present experiment, we have not measured the temperature dependence of any Bragg peak. Surprisingly, the first step increase in the temperature dependence of the Bragg peak intensity observed by Murani[20] is located around 130 K. We point out that this latter experiment corresponds to a q integration on $\Delta q = 0.1$ Å^{-1}, thus including a very small q contribution. At very small q, where the neutrons probe large inhomogeneities such as domain walls, the constant-q intensity increases just below T_c, according to the domain squared magnetization. This could provide a possible explanation for such a shift in the temperatures. The onset of static transverse spin components is predicted by several theoretical works (Gabay and Toulouse[26] and Parker and Saslow[31]) but a complete description of this "canted" state is still lacking. The observation of ferromagnetic correlations between transverse spins is not taken into account by any model. Moreover, below this temperature, several anomalous features are also observed that we summarize now. The hyperfine field measured by Mossbauer spectroscopy[32] for the $x = 0.19$ alloy shows a kink at 50–60 K, the electron paramagnetic resonance (EPR) linewidth[33] exhibits a maximum around 35–40 K below the minimum observed around 120 K, the Bragg peak 111($x = 0.19$) shows a second step increase around 50 K,[20] namely, close to the temperature where the spin-wave stiffness shows a minimum, and the susceptibility decreases below 26 and 38 K for the $x = 0.19$ and 0.21 samples, respectively.[31] A clear understanding of these effects and their possible relation with the "Almeida-Thouless" transition predicted below the Gabay-Toulouse transition by the mean-field approach is lacking.

ACKNOWLEDGMENTS

One of the authors (M. Hennion) is especially indebted to S. M. Maleev for enlightening discussions and to Björn Winkler for a critical reading of the manuscript.

[1]H. Maletta, G. Aeppli, and S. M. Shapiro, Phys. Rev. Lett. **48**, 1490 (1982).
[2]G. Gavoille and J. Hubsch, J. Phys. (Paris) Colloq. **49**, C8-1159 (1988).
[3]B. V. B. Sarkissian, J. Phys. F **11**, 2191 (1981).
[4]A. Razzaq and J. S. Kouvel, J. Appl. Phys. **55**, 1623 (1984).
[5]S. K. Burke and B. D. Rainford, J. Phys. F **13**, 441 (1983).
[6]Y. Yeshurun, M. B. Salamon, N. V. Rao, and H. S. Chen, Phys. Rev. Lett. **45**, 1366 (1980).
[7]D. Boumazouma, C. Tete, J. Durand, P. Mangin, and J. L. Soubeyroux, J. Magn. Magn. Mater. **54**, 95 (1986).
[8]J. A. Fernandez-Bacca, J. W. Lynn, J. J. Rhyne, and G. E. Fish, J. Appl. Phys. **63**, 3749 (1988).
[9]M. Hennion, I. Mirebeau, B. Hennion, S. Lequien, and F. Hippert, Europhys. Lett. **2**, 393 (1986).
[10]I. Mirebeau, S. Itoh, S. Mitsuda, T. Watanabe, Y. Endoh, M. Hennion, and R. Papoular, Phys. Rev. B **41**, 11 405 (1990); I. Mirebeau, M. Hennion, S. M. Mitsuda, and Y. Endoh, in *Recent Progress in Random Magnets,* edited by D. H. Ryan (World Scientific, Singapore, 1992).
[11]S. M. Shapiro, C. R. Fincher, A. C. Palumbo, and R. D. Parks, Phys. Rev. Lett. **45**, 474 (1980).
[12]G. Aeppli, S. M. Shapiro, R. J. Birgenau, and H. S. Chen, Phys. Rev. B **29**, 2589 (1984).
[13]R. W. Erwin, J. Lynn, J. J. Rhyne, and H. S. Chen, J. Appl. Phys. **57**, 3473 (1985).
[14]J. A. Fernandez Baca, J. J. Rhyne, G. E. Fish, M. Hennion, and B. Hennion, J. Appl. Phys. **67**, 5223 (1990).
[15]A. P. Murani, Phys. Rev. B **28**, 432 (1983).
[16]B. Hennion, M. Hennion, F. Hippert, and A. P. Murani, J.

Phys. F **14**, 489 (1984).
[17]B. Hennion, M. Hennion, I. Hennion, and F. Hippert, Physica B **136**, 49 (1986).
[18]M. Hennion, B. Hennion, I. Mirebeau, S. Lequien, and F. Hippert, J. Phys. (Paris) Colloq. **49**, C8-1121 (1988).
[19]A. P. Murani, S. Roth, P. Radakrishna, B. P. Rainford, B. R. Coles, K. Ibel, G. Goltz, and F. Mezei, J. Phys. F **6**, 425 (1976).
[20]A. P. Murani, Solid State Commun. **34**, 705 (1980).
[21]S. Mitsuda, H. Yoshisawa, T. Watanabe, S. Itoh, Y. Endoh, and I. Mirebeau, J. Phys. Soc. Jpn. **60**, 1721 (1991).
[22]F. Hartmann-Boutron, A. Ait-Bahammou, and C. Meyer, J. Phys. (Paris) **48**, 435 (1987).
[23]C. Lartigue, F. Mezei, C. Pappas, and M. Alba, Physica B **180** & **181**, 359 (1992).
[24]P. A. Lindgard, Phys. Rev. B **27**, 2980 (1983).
[25]D. Sherrington and S. Kirkpatrick, Phys. Rev. Lett. **35**, 1972 (1975).
[26]M. Gabay and G. Toulouse, Phys. Rev. Lett. **47**, 201 (1981).
[27]S. L. Guinsburg, Sov. Phys. JETP **49**, 1127 (1979).
[28]V. Feigelman and A. M. Tsvelik, Sov. Phys. JETP **37**, 901 (1979).
[29]M. A. Continentino, Phys. Rev. B **27**, 4351 (1983); S. V. Maleev and Yu. Skryabin, Sov. Phys. JETP **56**, 207 (1992).
[30]Ya. Korenblit, S. V. Maleev, and E. F. Shender, Phys. Rev. B **33**, 624 (1986).
[31]G. N. Parker and W. M. Saslow, Phys. Rev. B **38**, 11 718 (1988).
[32]F. Varret, A. Hamzic, and I. A. Campbell, Phys. Rev. B **26**, 5285 (1982).
[33]B. R. Coles, B. V. B. Sarkissian, and R. H. Taylor, Philos. Mag. B **37**, 789 (1978).